IOP Publishing Journal of Physics: Conference Series **61** (2007) 1294–1298
doi:10.1088/1742-6596/61/1/255 International Conference on Nanoscience and Technology (ICN&T 2006)

Magnetism induced by single-atom defects in nanographites

Oleg V Yazyev and Lothar Helm

Ecole Polytechnique Fédérale de Lausanne (EPFL),
Institute of Chemical Sciences and Engineering,
CH-1015 Lausanne, Switzerland

E-mail: oleg.yazyev@epfl.ch

Abstract. We study from first principles the magnetism in graphene induced by single carbon atom defects. For two types of defects considered in our study, the hydrogen chemisorption defect and the vacancy defect, the magnetism due to the defect-induced extended states has been observed. Calculated magnetic moments are equal to 1 μ_B per hydrogen chemisorption defect and $\sim$1.5 μ_B per vacancy defect. The magnetic ordering is either ferromagnetic or antiferromagnetic, depending on whether the defects correspond to the same or to different hexagonal sublattices of the graphene lattice, respectively.

The last two decades were marked with the discoveries of new allotropic modifications of carbon and related nanostructures. Graphene, the single two-dimensional sheet of graphite, is the starting point for many carbon nanomaterials, which are commonly called nanographites. These materials, being diverse in atomic structure, display a wide range of electronic properties. Magnetism of carbon materials [1] is of particular interest since in current technological applications magnetic materials are based on d and f elements. New carbon-based magnetic materials would greatly extend the limits of technologies relying on magnetism. Even more promising is the application of such materials in the design of nanoscale magnetic and spin electronics devices.

While ideal graphite and carbon nanotubes are in itself nonmagnetic, experimental observations of magnetic ordering are often explained by the presence of impurities [2], boundaries [3, 4] or defects [5, 6]. Defects in nanographites [7] can be created intentionally by irradiating material with electrons or ions [8, 9, 10, 11]. By manipulating the conditions of the irradiation it is possible to tune, in a flexible way, the properties of the carbon-based materials [12, 13, 14, 15]. Examples of simple defects in nanographites are single atom vacancies and hydrogen chemisorption defects. The former defect type is produced upon the irradiation with high energy particles [6] while the latter is the major outcome of the hydrogen plasma treatment [8]. The common feature of both types of defects is that only one carbon atom is removed from the π conjugation network of the graphene sheet. The single-atom defects on the graphene lattice give rise to quasilocalized states at the Fermi level [16, 8, 17, 18]. The graphene honeycomb lattice can be viewed as two interpenetrating hexagonal sublattices of carbon atoms commonly labeled as α and β. When a defect is created in the α lattice, only the p_z orbitals of carbon atoms in the β sublattice contribute to the quasilocalized state, and vice versa. These states extend over several nanometers around the defects forming characteristic $(\sqrt{3}\times\sqrt{3})R30^\circ$

superstructures recognized in STM images. Analyzing the position and the orientation of the superstructures one can precisely locate the defect and determine the sublattice to which it belongs [16, 19]. The fact that quasilocalized states lie at the Fermi level suggests that magnetism can be induced by the electron exchange instability.

Using first principles approaches we investigate magnetism originating from the quasilocalized states induced by single-atom point defects in graphene. The results obtained can eventually be extended, with some precautions, to defects in other nanographites. The model system consists of a periodic two-dimensional superlattice of defects in graphene. The supercell size can be varied resulting in different distances d between the neighbor defects on the superlattice and in different defect concentrations. For our supercell definition the resulting distance between neighbor defects is about $3na_{cc}$ where a_{cc}=1.42 Å is the C-C distance in graphene. The corresponding number of carbon atoms per unit cell is $6n^2$. Our investigation is restricted to the cases with n=2−6. The largest system we considered is characterized by about 25 Å separation between neighbor defects, which corresponds to a defect concentration of 0.5%.

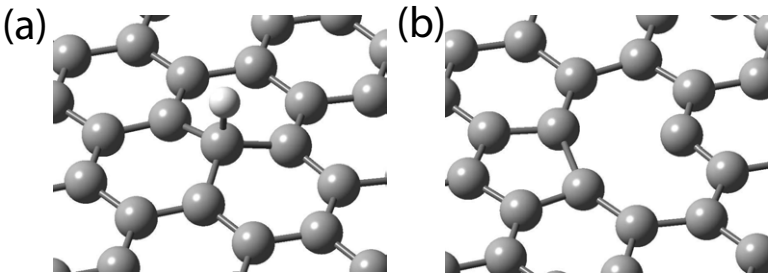

Figure 1. Atomic structures of the hydrogen chemisorption defect (a) and the vacancy defect (b) in graphene.

Density functional theory calculations were performed using the `SIESTA` code [20]. The generalized gradient approximation exchange-correlation density functional of Perdew, Burke and Ernzerhof (PBE) [21] was employed. All calculations were performed in the spin-unrestricted manner using the diagonalization-based method for solving Kohn-Sham equations. The shifted Monkhorst-Pack grids [22] corresponding to a cutoff of 100 a. u. were used to sample the Brillouin zone in two dimensions. Atomic positions and cell dimensions were relaxed. The numerical atomic orbital basis set of single-ζ plus one polarization function quality and double-ζ plus one polarization function quality have been used throughout the study.

In the following we present our results for the two types of defects mentioned above. The structure of the hydrogen chemisorption defect is shown in Fig. 1a. This defect is characterized by the slight protrusion of the hydrogenated carbon atom and the very small displacement of all other neighbor carbon atoms [23, 24]. The single atom vacancy defect in graphene is nearly planar (Fig. 1b). The local three-fold symmetry breaks down due to the Jahn-Teller distortion induced by the reconstruction of two dangling bonds left after removing the carbon atom. This gives rise to the in-plane displacement of other carbon atoms in the graphene lattice [25, 6]. The third dangling bond is left unsaturated providing a contribution of magnitude 1 μ_B to the intrinsic magnetic moment of the defect.

Magnetism induced by the presence of the quasilocalized defect states $\psi_d(\vec{r})$ has been observed for both defect types. The hydrogen chemisorption defect gives rise to the strong Stoner ferromagnetism [26] with a magnetic moment of 1 μ_B per defect at all studied concentrations. The flat defect bands give rise to the narrow peaks at the Fermi level (Fig. 2a) which is close to this of the ideal graphene. The defect band maxima for the majority spin and the minority spin components lie, respectively, lower and higher than the the Fermi levels for both defective and ideal graphene. This leads to the conclusion that the hydrogen chemisorption motif is charge neutral and spin-polarized in the wide range of defect concentrations. On the contrary, fractional magnetic moments and weak ferromagnetism have been observed for the vacancy-type defect

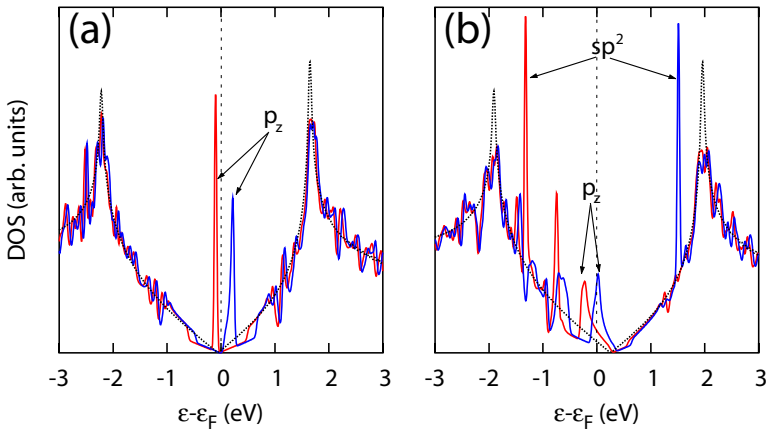

Figure 2. Spin-resolved density of states plots for the systems with the hydrogen chemisorption defects (a) and with the vacancy defects (b) ($n = 4$). Red color refers to the majority spin density, blue color refers to the minority spin density. The dotted line shows the density of states of the ideal graphene. Labels indicate the character of the defect states.

models. For 0.5–4% defect concentrations the magnetic moment was found to vary in the range of 1.45−1.53 μ_B. For the vacancy-type defect, the total magnetic moment is determined by the contribution (1 μ_B) of the localized sp^2 dangling bond state and the contribution (<1 μ_B) of the extended defect state, $\psi_d(\vec{r})$. The fractional spin polarization of $\psi_d(\vec{r})$ is explained by the self-doping (charge transfer from the bulk to $\psi_d(\vec{r})$), which arise from the stabilization of the defect state. The stabilization of vacancy defect extended states is possible in the case of a significant coupling between the second nearest neighbor atoms belonging to the same sublattice [18]. In the case of the vacancy defect, the indirect coupling is justified by the formation of the covalent bond between the two carbon atoms that follows the defect reconstruction. No such bond is possible in the case of hydrogen chemisorption. Therefore, we conclude that the character of the magnetism induced by the defects depend on their local structure. The defect state exchange splitting, defined as the difference between the corresponding majority spin and minority spin band maxima, decreases as the defect concentration decreases. This is not surprising since the degree of the localization of the defect states depends on the defect concentration [18]. At the lowest studied defect concentration of 0.5%, the exchange splitting were found to be 0.23 eV and 0.14 eV for the hydrogen chemisorption and vacancy defects, respectively. At low concentrations the magnetism in defective nanographites is expected to be sensitive to the variations of the Fermi energy resulting from self-doping, presence of other defects or applied bias, and to the disorder-induced broadening.

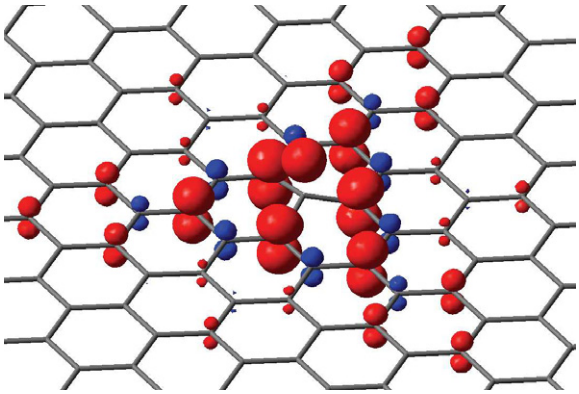

Figure 3. Isosurface representation of the spin density distribution around the hydrogen chemisorption defect. Red color refers to the majority spin density, blue color refers to the minority spin density.

The distributions of the electron spin magnetization density in the vicinity of both types of defects clearly show the characteristic $\sqrt{3}\times\sqrt{3}$ patterns also observed for the charge density in the STM experiments. For the hydrogen chemisorption defect the spin density distribution

(Fig. 3) clearly shows the three-fold symmetry. The distribution of the electron spin density is represented in Fig. 4a (n=6 model) by means of the Mulliken spin populations averaged over ith nearest neighbors to the defect atom. The spin populations show a dumped oscillation behavior as a function of the nearest neighbor index and, therefore, of the distance to the defect. The magnetization pattern is explained by the fact that the defect state is distributed over the sites of the sublattice complementary to the one in which the defect was created (i. e. over the odd nearest neighbors), and shows a power law decay [18]. The major positive contribution to the electron spin density is defined by the exchange splitting of the defect states. In addition, the exchange spin-polarization effect (i.e. the response of the fully populated valence bands to the magnetization of the defect states) results in a negative spin density on the even nearest neighbor sites (blue in Fig. 3) and in the enhancement of a positive spin density on the odd nearest neighbor sites (red in Fig. 3). A similar phenomenon takes place in the case of the neutral bond length alternation defect states in one-dimensional polyene chains [27, 28]. The calculated magnitude of the negative spin-polarization is ∼1/3 of the positive spin populations on the neighbor sites in the vicinity of the defect site. This is close to the ratio observed for the *trans*-polyacetylene [27]. The magnitudes of the spin populations are lower in the case of the vacancy defect because of the fractional spin-polarization of the defect band.

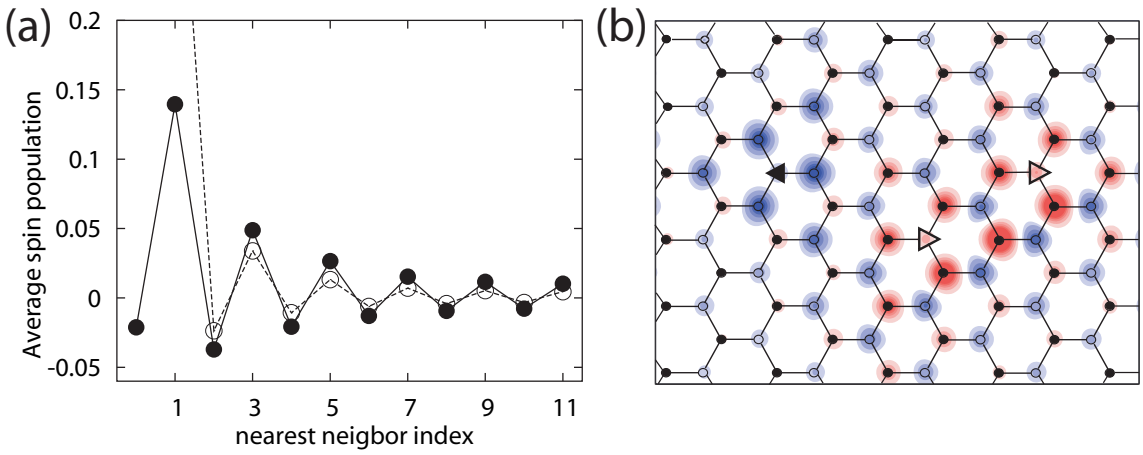

Figure 4. (a) Dependence of the spin populations averaged over ith nearest neighbors of the hydrogen chemisorption defects (•) and the vacancy defects (○). (b) Projection of the sin density distribution in the system with three hydrogen chemisorption defects (two defects in sublattice α (▷) and one in sublattice β (◀)).

According to the Stoner picture, the magnetic ordering is driven by the exchange energy $E_x \sim -\sum_i M_j^2$ with M_j being the magnetization of the p_z orbital of the jth carbon atom [26]. Ferromagnetic ordering is the only possibility for the magnetism originating from quasilocalized states induced by defects in the same sublattice because of the non-oscillating behavior of both M_j within the same sublattice and the indirect coupling due to the semimetallic properties of graphene [29]. On the contrary, for the case of defect states in different sublattices, E_x is minimized when the coupling is antiferromagnetic. In this case, the mechanism of the exchange coupling is defined by the indirect spin-polarization effect. To illustrate this point, we calculated the ground state magnetic configuration of the system with three close hydrogen chemisorption defects using the DFT approach. We found that in the ground state configuration two defects in the α sublattice are coupled ferromagnetically with each other and antiferromagnetically with the third defect in the β sublattice (Fig. 4b). The resulting magnetic moment of this system amount to 1 μ_B, and the characteristic $\sqrt{3}\times\sqrt{3}$ superstructure patterns of the magnetization

density associated with individual defects can be recognized. In nanographite materials with defects present with an equal probability in both sublattices, the overall correlation of the magnetic moments is expected to be antiferromagnetic. The antiferromagnetic ordering was experimentally observed in carbon nanohorns [30, 31].

In conclusion, our calculations reveal the itinerant-like mechanism of the magnetism triggered by simple irradiation-induced point defects in graphene. It is notable, that the magnetism develops even in the absence of the unsaturated dangling bonds as it was shown for the case of the hydrogen chemisorption defect. Both ferromagnetic and antiferromagnetic scenarios of the magnetic correlation are possible. Moreover, for the two types of defects investigated in our work the character of magnetism was found to be different. This will permit versatile tailoring of magnetic materials and nanostructures for future technological applications.

Authors acknowledge G. Buchs, D. Ivanov and I. Tavernelli for discussions. O. Y. thanks the Swiss National Science Foundation for financial support. The computational resources were provided by the Swiss Center for Scientific Computing and the DIT-EPFL.

References

[1] Makarova T and Palacio F (eds.) 2005 *Carbon-Based Magnetism: An Overview of Metal Free Carbon-Based Compounds and Materials* (Amsterdam: Elsevier)
[2] Coey J M D, Venkatesan M, Fitzgerald C B, Douvalis A P and Sanders I S 2002 *Nature* **420** 156
[3] Okada S and Oshiyama A 2001 *Phys. Rev. Lett.* **87** 146803
[4] Lee H, Son Y-W, Park N, Han S and Yu J 2005 *Phys. Rev. B* **72** 174431
[5] Kim Y-H, Choi J, Chang K J and Tománek D 2003 *Phys. Rev. B* **68** 125420
[6] Lehtinen P, Foster A S, Ma Y, Krasheninnikov A and Nieminen R M 2004 *Phys. Rev. Lett.* **93** 187202
[7] Charlier J-C 2002 *Acc. Chem. Res.* **35** 1063
[8] Ruffieux P, Gröning O, Schwaller P, Schlapbach L and Gröning P 2000 *Phys. Rev. Lett.* **84** 4910
[9] Esquinazi P, Spemann D, Höhne R, Setzer A, Han K-H and Butz T 2003 *Phys. Rev. Lett.* **91** 227201
[10] Hashimoto A, Suenaga K, Gloter A, Urita K and Iijima S 2004 *Nature* **430** 870
[11] Urita K, Suenaga K, Sugai T, Shinohara H and Iijima S 2005 *Phys. Rev. Lett.* **94** 155502
[12] Banhart F 1999 *Rep. Prog. Phys.* **62** 1181
[13] Mikó C, Milas M, Seo J W, Couteau E, Barisic N, Gaál R and Forró L 2003 *Appl. Phys. Lett.* **83** 4622
[14] Han K-H, Stepmann D, Esquinazi P, Höhne R, Riede V and Butz T 2003 *Adv. Mater.* **15** 1719
[15] Kis A, Csányi G, Salvetat J-P, Lee T-N, Couteau E, Kulik A J, Benoit W, Brugger J and Forró L 2004 *Nat. Mater.* **3** 153
[16] Mizes H A and Foster J S 1989 *Science* **244** 559
[17] Ruffieux P, Melle-Franco M, Gröning O, Bielmann M, Zerbetto F and Gröning P 2005 *Phys. Rev. B* **71** 153403
[18] Pereira V M, Guinea F, dos Santos J M B L, Peres N M R and Castro Neto A H 2006 *Phys. Rev. Lett.* **96** 036801
[19] Kelly K and Halas N 1998 *Surf. Sci.* **416** L1085
[20] Soler J M, Artacho E, Gale J D, García A, Junquera J, Ordejón P and Sánchez-Portal D 2002 *J. Phys.: Condens. Matter* **14** 2745
[21] Perdew J P, Burke K and Ernzerhof M 1996 *Phys. Rev. Lett.* **77** 3865
[22] Monkhorst H J and Pack J D 1976 *Phys. Rev. B* **16** 5188
[23] Ruffieux P, Gröning O, Bielmann M, Mauron P, Schlapbach L and Gröning P 2002 *Phys. Rev. B* **66** 245416
[24] Duplock E J, Scheffler M and Lindan P J D 2004 *Phys. Rev. Lett.* **92** 225502
[25] Lu A J and Pan B C 2004 *Phys. Rev. Lett.* **92** 105504
[26] Mohn P 2003 *Magnetism in the solid state* (Berlin Heidelberg: Springer-Verlag)
[27] Thomann H, Dalton L R, Tomkiewicz Y, Shiren N S and Clarke T C 1983 *Phys. Rev. Lett.* **50** 533
[28] Kirtman B, Hasan M and Chipman D M 1991 *J. Chem. Phys.* **95** 7698
[29] Vozmediano M A H, López-Sancho M P, Stauber T and Guinea F 2005 *Phys. Rev. B* **72** 155121
[30] Garaj S, Thien-Nga L, Gaál R, Forró L, Takahashi K, Kokai F, Yudasaka M and Iijima S 2000 *Phys. Rev. B* **62** 17115
[31] Imai H, Babu P K, Oldfield E, Wieckowski A, Kasuya D, Azami T, Shimakawa Y, Yudasaka M, Kubo Y and Iijima S 2006 *Phys. Rev. B* **73** 125405